2013 IEEE/RSJ International Conference on
Intelligent Robots and Systems (IROS)
November 3-7, 2013. Tokyo, Japan

Prediction-Based Interception Control Strategy Design with a Specified Approach Angle Constraint for Wheeled Service Robots

Wanfeng He, Yongchun Fang, *Senior Member, IEEE*, Xuebo Zhang, *Member, IEEE*

***Abstract*—This paper designs an innovative prediction-based interception control strategy to enable a wheeled mobile robot to intercept a dynamic target with a specified angle, which can be potentially utilized in such applications as service robots. Specifically, visual information is collected and then utilized to estimate the state of the moving target, based on which, the follow-up pose of the target is calculated so as to improve the interception accuracy. A prediction-based controller is then proposed to drive the wheeled robot to efficiently intercept a dynamic target with a specified angle, whose stability is proven by Lyapunov techniques. Both simulation and experimental results are provided to demonstrate the superior performance of the proposed approach.**

I. Introduction

Interception, especially with a specified angle, is a very important task in numerous applications, such as active surveillance and automatic service by wheeled mobile robots. In order to develop effective methods for this task, several challenges including target detection, controller design and state estimation, must be taken into account. Wherein, interception control strategy largely determines whether the service robot can successfully accomplish the task or not. Therefore, many different control approaches have been proposed in the literature to solve various target interception problems, considering different target motion characteristics as well as the robot kinematic models.

Navigation and guidance methods have been widely employed in dynamic target interception and tracking tasks [1], [2], [3], [4]. Common methods for navigation guidance, such as PNG (Proportional Navigation Guidance), APNG (Augmented Proportional Navigation Guidance), IPNG (Ideal Proportional Navigation Guidance) and AIPNG (Augmented Ideal Proportional Navigation Guidance), are applied to the problem of intercepting a moving object in real-time by using an industrial robotic manipulator. Further, these methods, when combined with some trajectory tracking algorithms, can ensure smooth interception. However, unlike a manipulator, a wheeled mobile robot is subject to nonholonomic constraint, which largely increases the complexity of the interception task when a mobile robot is utilized as an interceptor. Also considering about the requirement of a specified interception angle, the aforementioned methods can be hardly extended to enable a mobile robot to implement the interception task with a given angle. Based on this observation, [5] and [6] develop a mobile robot navigation technique, named as CNG (Circle Navigation Guidance) algorithm, to intercept a moving target with a specific angle. The guidance law is obtained by converting the finite-time navigation problem into a task of maintaining a certain geometric condition at all times. However, due to the limitation of robot turn radius caused by the limited steering angle and the nonholonomic constraint, the interception strategy cannot meet the requirements in many situations.

This work is supported by National Natural Science Foundation of China (Grant No.61203333), Specialized Research Fund for the Doctoral Program of Higher Education of China (Grant No.20120031120040), and and Tianjin Natural Science Foundation (Grant No. 13JCQNJC03200).

W. He, Y. Fang (corresponding author) and X. Zhang are with Institute of Robotics and Automatic Information System and Tianjin Key Laboratory of Intelligent Robotics, Nankai University, Tianjin 300071, China (e-mail: yfang@robot.nankai.edu.cn, zhangxb@robot.nankai.edu.cn, hewf@robot.nankai.edu.cn)

Path and motion planning methods [7], [8], [9] are also widely utilized for moving target interception. This kind of approach generally utilizes the time parametric function of the moving object to generate an interception trajectory for the mobile robot to track; hence, it is only effective to intercept slow-maneuvering objects with limited acceleration, because massive data processing consumption on trajectories generation remarkably reduces the real-time performance of the interception system.

For most interception tasks, the motion of the dynamic target is usually unknown in advance, thus, visual feedback [10] and line-of-sight methods [11], [12] have been proven as effective approaches for the interception task. Furthermore, omni-directional vision systems are employed in [13], [14], [15] to determine the robot pose from extracted features, so that some basic operations for a soccer robot can be implemented in terms of trajectory tracking and pose stabilization. On the other hand, human-like strategies have been more and more often utilized in the interception problem with mobile robots. These works adopt some human-like behaviors, such as anthropomorphic driving, to accomplish interception tasks more wisely [16], [17]. Yet, this method is usually empirical, and there is no theoretical guarantee for the performance of this kind of interception systems.

The interception control strategy proposed in this paper aims to enable a wheeled service robot to provide some service for a human being. To this end, the interception needs to be implemented with a specific angle, such as head-on interception, and the interception efficiency is of extreme importance. Motivated by these facts, we propose a novel prediction-based scheme in this paper to achieve an efficient interception for a dynamic target with some specific angle to meet the service requirements. Specifically, the proposed approach employs visual information to estimate the state of the dynamic target and then makes short-term predictions for the target motion. The obtained information is subsequently utilized by the designed control law to implement efficient interception.

II. Problem Development

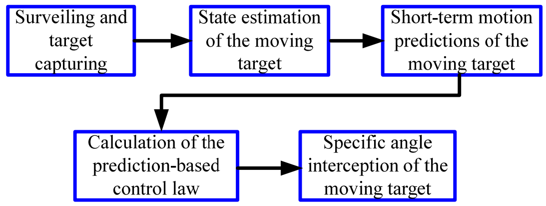

Fig. 1. The procedure of the pedestrian interception method.

As shown in Fig. 1, for the pedestrian interception task, the robot keeps surveilling its service region, and whenever any possible dynamic target appears, the robot, with the aid of the on-board PTZ-camera, starts to recognize the target and then intercepts it efficiently to provide some pre-defined service. To achieve this objective, the interception system is divided into three main functional modules. Firstly, if a dynamic object is captured as the interested target, the orientation of the camera will be controlled to enable visual tracking for the target. Secondly, based on some human detection algorithm and geometrical analysis, the depth of the target will be estimated instantly. After that, visual measurement of the target is utilized by the Extended Kalman filter to calculate the states of the dynamic target, including its pose and velocity, which are employed to implement short-term prediction for the movement of the target. Thirdly, a novel prediction-based control scheme, which integrates all of the above information, is designed to enable the robot to intercept the target from a specific angle efficiently and accurately. It should be noted that this paper mainly focuses on the steps of state estimation/prediction and the interception controller design, while the details for visual tracking are beyond the scope of this paper.

III. State Estimation-Based Pose Prediction of the Moving Target

In this section, a vision-based state estimation method is proposed, wherein the resulting depth and velocity of the target will be utilized to facilitate the subsequent pose prediction of the moving target.

A. Kinematic Model and Velocity Estimation

For the interception task, the velocity information of the dynamic target with respect to the robot is required to enable feedback control to successfully drive the robot to block the way of the target. Unfortunately, the velocity of the target is generally unavailable from the on-board sensors. To solve this problem, we establish the kinematic model of the target with respect to the robot reference frame, based on which the Extended Kalman filtering technique is then employed to estimate the target's relative velocity by the utilization of visual measurements.

The relative relationship between the robot and the target is shown in Fig. 2, where F_W and F_R denote the world and the robot frames, respectively. The solid and the dotted line triangles represent the current position and the follow-up prediction of the target, respectively.

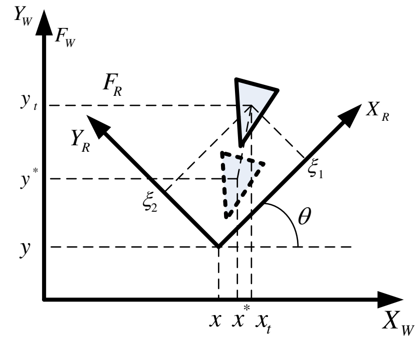

Fig. 2. The geometric relationship of the robot and the target.

The kinematic model of the mobile robot and the target can be described as:

$$\begin{cases} \dot{x} = v\cos\theta \\ \dot{y} = v\sin\theta \\ \dot{\theta} = \omega \end{cases}, \quad \begin{cases} \dot{x}_t = v_{tx} \\ \dot{y}_t = v_{ty} \end{cases} \tag{1}$$

where (x, y) are the coordinates of the origin (the center of the robot) of F_R expressed in the frame F_W, (x_t, y_t) represent the coordinates of the target in the frame F_W, θ is the intersection angle of the X_R axis and the X_W axis, v and ω are the linear and angular velocities of the robot, v_t is the velocity of the target in F_W, which can be decomposed into v_{tx} and v_{ty} along the corresponding axes in F_W. Based on Fig. 2, the geometric relationship between the robot and the target can be obtained:

$$\begin{cases} x_t = x + \xi_1\cos\theta - \xi_2\sin\theta \\ y_t = y + \xi_1\sin\theta + \xi_2\cos\theta \end{cases}, \tag{2}$$

where (ξ_1, ξ_2) are the coordinates of the target in the robot frame F_R.

By solving the constraint (2), the relative position of the target with respect to the robot can be calculated as:

$$\begin{cases} \xi_1 = (x_t - x)\cos\theta + (y_t - y)\sin\theta \\ \xi_2 = (-x_t + x)\sin\theta + (y_t - y)\cos\theta \end{cases}. \tag{3}$$

After taking the time derivative of (3), we obtain:

$$\begin{cases} \dot{\xi}_1 = v_{tx}\cos\theta + v_{ty}\sin\theta - v + \omega\xi_2 \\ \dot{\xi}_2 = -v_{tx}\sin\theta + v_{ty}\cos\theta - \omega\xi_1 \end{cases}. \tag{4}$$

However, the velocity of the target used in the interception controller is expressed in F_R, therefore, we need to convert (4) into appropriate equations expressed in F_R. To this end, v_{tx} and v_{ty} are mapped from F_W to F_R to deduce the following equations:

$$\begin{cases} v_{tx}^R = v_{tx}\cos\theta + v_{ty}\sin\theta \\ v_{ty}^R = -v_{tx}\sin\theta + v_{ty}\cos\theta \end{cases}, \tag{5}$$

where v_t^R is the velocity of the moving target expressed in F_R, which can be decomposed into v_{tx}^R and v_{ty}^R along corresponding axes.

Finally, the kinematic model of the target with respect to the robot reference frame F_R can be obtained by combining (4) and (5) as follows:

$$\begin{cases} \dot{\xi}_1 = v_{tx}^R - v + \omega\xi_2 \\ \dot{\xi}_2 = v_{ty}^R - \omega\xi_1 \end{cases}. \tag{6}$$

So far, we have obtained the state equations for the estimated variables, which are explicitly expressed as:

$$\begin{bmatrix} \dot{v}_{tx}^R \\ \dot{v}_{ty}^R \\ \dot{\xi}_1 \\ \dot{\xi}_2 \end{bmatrix} = \begin{bmatrix} 0 \\ 0 \\ v_{tx}^R - v + \omega\xi_2 \\ v_{ty}^R - \omega\xi_1 \end{bmatrix} + w(t), \tag{7}$$

where $\omega(t)$ is the process noise and it is usually assumed that $\dot{v}_{tx}^R \approx 0, \dot{v}_{ty}^R \approx 0$. (ξ_1, ξ_2) is calculated from the image feature points with some geometric relationship and the estimated depth between the target and the mobile robot. The depth estimation method, together with some convincing experiment results, is discussed in [18].

Based on equation (7), the Extended Kalman filtering technique can be employed to process the visual signals, so as to estimate the velocity of the target.

B. Pose Prediction of the Moving Target

The pose prediction step aims to make the interception more efficiently and more accurately. When the relative distance and the velocity information of the moving target are obtained, its follow-up pose can be predicted based on its kinematics. The predicted position of the moving target will be set as the interception location, and the robot will be controlled to move towards this location to implement the specific angle interception.

According to (2), the predicted position (x^*, y^*) can be obtained by adding an increment to its current position (x, y):

$$\begin{cases} x^* = x + (\xi_1 + \Delta\xi_1)\cos\theta - (\xi_2 + \Delta\xi_2)\sin\theta \\ y^* = y + (\xi_1 + \Delta\xi_1)\sin\theta + (\xi_2 + \Delta\xi_2)\cos\theta \end{cases}, \tag{8}$$

where $\Delta\xi_1 = \dot{\xi}_1 nT$ and $\Delta\xi_2 = \dot{\xi}_2 nT$, $n \in N^+$ will be chosen according to the actual needs, T represents the system sampling period, and the target velocity $(\dot{\xi}_1, \dot{\xi}_2)$ has been successfully estimated previously.

IV. Interception Controller Design and AnalysiS

The objective of this section is to design a prediction-based controller to enable a wheeled robot to efficiently intercept a dynamic target with a specified angle. In particular, we take the kinematic model of the nonholonomic mobile robot as:

$$\begin{cases} \dot{x} = v\cos\theta \\ \dot{y} = v\sin\theta \\ \dot{\theta} = \omega \end{cases}, \tag{9}$$

where $\vec{P} = [x, y, \theta]^T$ is the robot pose expressed in the world frame F_W (see Fig. 2), v and ω are the robot linear and angular velocities.

A. Interception Controller Design

As mentioned previously, the succedent pose of the target can be predicted from the estimated state information, and the prediction of the moving target is set as the desired location for the next step, then an interception controller is needed to make the robot move toward the required pose to implement the interception with the previously specified angle. In this case, the angular velocity needs to insure that the robot converges to the assigned orientation with respect to the target during the robot's motion process. The current and desired pose of the robot is shown in Fig. 3. It should be noted that such a way of intercepting a moving target can enable the robot to provide some possible service or send messages to the target with a more polite manner, which is apparently different from the conventional trajectory tracking problem.

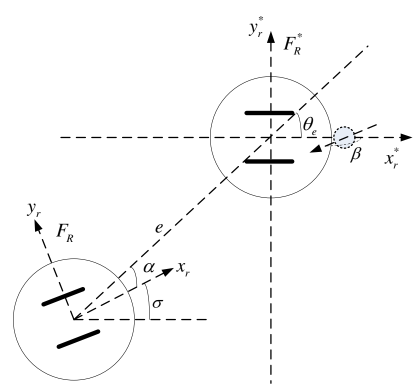

Fig. 3. The current and desired pose of the robot.

In Fig. 3, F_R and F_R^* denote the current and the desired robot frames, respectively. It should be noted that the desired position has been set as the prediction of (x^*, y^*), so as to lead the robot to implement efficient interception.

To facilitate the design of the interception control law, the distance error $e(t)$ between the robot's current and desired positions is calculated from (9) as follows:

$$\begin{aligned} e &= \sqrt{(x^* - x)^2 + (y^* - y)^2} \\ &= \sqrt{(\xi_1 + \dot{\xi}_1 T)^2 + (\xi_2 + \dot{\xi}_2 T)^2} \end{aligned} . \quad (10)$$

Also, the intersection angle $\theta_e(t)$ between the orientation of the robot's desired pose and the distance line $e(t)$ can be obtained as:

$$\theta_e = \arctan 2((\xi_2 + \dot{\xi}_2 T), (\xi_1 + \dot{\xi}_1 T)) . \quad (11)$$

The intersection angle $\sigma(t)$ of the robot's current and desired orientation can be calculated as:

$$\sigma = \arctan 2(-v_{ty}^R, -v_{tx}^R) + \beta , \quad (12)$$

where β is the desired interception angle which is formed by the predicted orientation of the target and the desired orientation of the robot. It should be set according to different tasks. When $\beta \in (-\frac{\pi}{2}, \frac{\pi}{2})$, this condition is known as the head-on interception. The intersection angle $\alpha(t)$ between the orientation of the robot's current pose and the distance line $e(t)$ can be obtained through the relationship of $\alpha(t) = \theta_e(t) - \sigma(t)$, as shown in Fig. 3.

After some mathematical calculation, the open-loop error system can be obtained as:

$$\begin{cases} \dot{\theta}_e = v \sin\alpha / e \\ \dot{\alpha} = -\omega + v \sin\alpha / e \\ \dot{e} = -v\cos\alpha \end{cases} . \quad (13)$$

Based on the open-loop dynamics, the interception controller is designed by using the available feedback signals and the estimated information:

$$\begin{cases} v = k_1 e \cos\alpha + k_1 | v_t^R | e \cos^2\sigma \cos\alpha \\ \omega = k_2\alpha + k_1 \cos\alpha \sin\alpha (1 + \frac{\theta_e}{\alpha})(1 + | v_t^R | \cos^2\sigma) \end{cases} , \quad (14)$$

where $k_i \in R^+, i = 1, 2$ denote positive control gains.

After substituting the control inputs (14) into the open-loop error system (13), the closed-loop error system can be obtained as:

$$\begin{cases} \dot{\theta}_e = k_1 \sin\alpha\cos\alpha + k_1 | v_t^R | \sin\alpha\cos\alpha\cos^2\sigma \\ \dot{e} = -k_1 e\cos^2\alpha - k_1 | v_t^R | e \cos^2\alpha\cos^2\sigma \\ \dot{\alpha} = -k_2\alpha - k_1\theta_e \sin\alpha\cos\alpha(1 + | v_t^R | \cos^2\sigma)/\alpha \end{cases} . \quad (15)$$

In fact, there is a problem of singularity at the origin in the closed-loop error system. To address this problem, $\omega(t) = k_1(1 + | v_t^R | \cos^2\sigma)\theta_e(t)$ is employed to control the robot when the distance error $e(t)$ is within a sufficient small range.

B. Stability Analysis

Theorem 1: The proposed controller (14) drives the nonholonomic mobile robot to its desired pose in the sense that:

$$\lim_{t\to\infty} e = 0, \lim_{t\to\infty} \alpha = 0, \lim_{t\to\infty} \theta_e = 0 . \quad (16)$$

Proof: The Lyapunov function candidate is taken as:

$$V = \frac{1}{2}e^2 + \frac{1}{2}\alpha^2 + \frac{1}{2}\theta_e^2 \geq 0 . \quad (17)$$

After some mathematical analysis, its time derivative is obtained as

$$\begin{aligned} \dot{V} &= e\dot{e} + \alpha\dot{\alpha} + \dot{\theta}_e\theta_e \\ &= v(-\cos\alpha e + \alpha\frac{\sin\alpha}{e} + \theta_e\frac{\sin\alpha}{e}) - \omega\alpha \\ &= -k_1 e^2\cos^2\alpha - k_1 | v_t^R | e^2 \cos^2\sigma\cos^2\alpha - k_2\alpha^2 \\ &\leq 0 \end{aligned} . \quad (18)$$

Then, it is concluded from (17), (18) and the first equation of (15) that

$$e(t), \alpha(t), \theta_e(t) \in \mathcal{L}_\infty . \quad (19)$$

Let Φ be the set of all points such that $\dot{V} = 0$, that is

$$\Phi = \{(e, \alpha, \theta_e) : \dot{V} = 0\} . \quad (20)$$

Hence, from (17) and (18), Barbalat's Lemma can be employed to show that

$$e = 0, \alpha = 0 . \quad (21)$$

It follows from (21) that in the set Φ, the following relationship holds:

$$\dot{e} = 0, \dot{\alpha} = 0 . \quad (22)$$

Substituting (21) and (22) into the third equation of (15) yields that

$$k_1(1 + | v_t^R | \cos^2\sigma)\theta_e = 0 . \quad (23)$$

Since $k_1, | v_t^R | > 0$, it follows from (23) that $\theta_e = 0$. Therefore, it is clear that the largest invariant set M in Φ only includes the equilibrium point in the sense that

$$M = \{e = 0, \alpha = 0, \theta_e = 0\} . \quad (24)$$

Based on the LaSalle's invariance principle, the system state converges to the origin asymptotically in the sense that $\lim_{t\to\infty} e(t) = 0, \lim_{t\to\infty} \alpha(t) = 0, \lim_{t\to\infty} \theta_e(t) = 0$.

According to Theorem 1, the error of the closed-loop system converges to zero asymptotically. To ensure the safety of the pedestrian, v is set to be zero when the depth $d(t)$ is smaller than a pre-defined safe threshold, making the controller of $\omega(t)=k_1(1+|v_t^R|\cos^2\sigma)\theta_e(t)$ successfully regulate the orientation of the robot. In this sense, singularity never happens and it thus will not affect the interception result.

V. SIMULATION AND EXPERIMENTS

In this section, some simulation and experiments are carried out to verify the performance of the proposed controller.

A. Simulation Results

In the simulation, the desired interception angle is set as $\beta=0$ for a head-on interception task. After that, the robot starts to supervise its service region. At this time, a pedestrian who will be served comes into the robot's vision, the robot automatically recognizes it and begins to implement the head-on interception task. When the distance between the target and the robot reaches the desired value, the robot stops near the target to accomplish the assigned tasks.

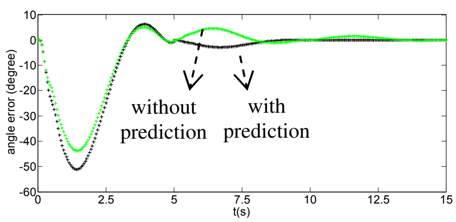

(a) Angle errors for straight-line target interception. Black curve: with prediction. Green curve: without prediction.

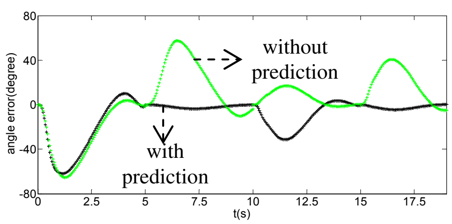

(b) Angle errors for sinusoidal-line target interception. Black curve: with prediction. Green curve: without prediction.

Fig. 4. Comparison of interception algorithms with/without prediction.

The simulation results for the interception algorithms with/without prediction are presented in Fig. 4, with Fig. 4(a) and Fig. 4(b) plotting the angle errors for the interception of straight-line target and sinusoidal-line target, respectively. It can be seen that the prediction-based interception algorithm exhibits much better performance, in the sense of fast convergence and small angle error indicating higher efficiency and accuracy.

Further, table I is provided to summarize the performance comparison for the interception algorithms with/without prediction part, where the simulation settings, such as initial pose of the mobile robot, the desired interception angle, and the distance between the robot and the pedestrian, are all set the same. In Table I, angle error and arrival time, which respectively indicates interception accuracy and efficiency, are selected as performance indices for the comparison. It can be seen from these results that the interception algorithm with prediction provides much better performance for different walking type pedestrians.

TABLE I. PERFORMANCE COMPARISON

Trajectory type of the pedestrian	Angle error(degree) with/without prediction	Arrival time(second) of the head-on angle with/without prediction
Straight	0/0~3	8/14
Sine (low frequency)	3~5/8~15	15/18
Sine (high frequency)	15/20~30	11/16
Circle	5~10/10~15	20/24

B. Experiment Results

A pedestrian interception experiment is carried out to fully demonstrate the performance of the interception system. To facilitate comparison, the experimental conditions are set identical to those of simulation test. That is, a pedestrian suddenly appears and walks into the scenario. As shown in Fig. 5, the pedestrian walks in a straight line, after capturing and recognizing the target, the robot is driven to intercept the pedestrian and stops in front of him successfully.

To gain a deeper understanding of the proposed algorithm, the experimental results are compared with those of the previous simulation test. The comparison of the robot's velocity is recorded in Fig. 6, where the blue and red curves represent the simulation data and the experimental results from the encoder, respectively. As shown in the figure, the experimental results accord well with those of the simulation test, yet there is still some mismatch between these two curves, which mainly comes from the mechanical flaw of the system and the noise of the encoder measurement. The curves shown in Fig. 7 and Fig. 8 represent the convergence process of $e(t)$ and $\alpha(t)$, where the steady-state errors are primarily caused by the visual measurement inaccuracy.

Fig. 5. Image series of the interception experiment.

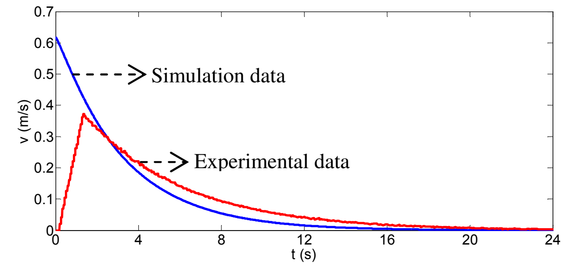

(a) The comparison of the robot's linear velocity.

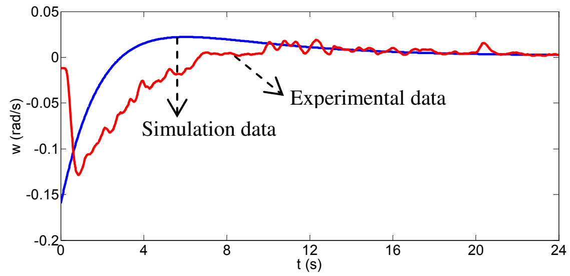

(b) The comparison of the robot's angular velocity.

Fig.6. A comparison of simulation and experiment results.

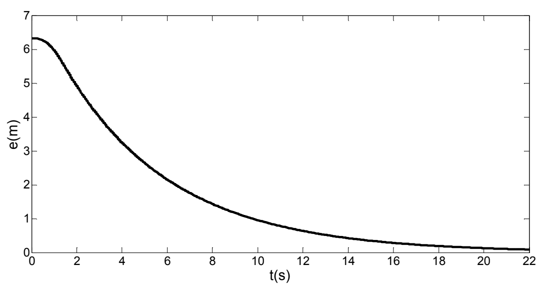

Fig.7. The convergence curve of $e(t)$.

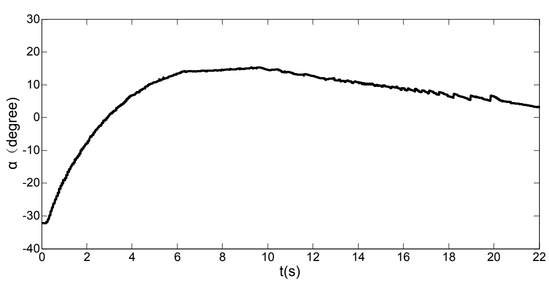

Fig.8. The convergence curve of $\alpha(t)$.

VI. Conclusion and Future Work

In this paper, we have presented a vision-based pedestrian interception approach consisting of state estimation and controller design. The proposed scheme has been validated through both simulation and experiment tests on a wheeled mobile robot, confirming its great applicability for service robots. For the future research, the navigation and path/motion planning techniques with some smarter strategies will be integrated into the interception system, and we are also trying to improve the target's state estimation performance by designing more ambitious algorithms.

References

[1] K. Karydis, L. Valbuena, H.G. Tanner, "Model Predictive Navigation for Position and Orientation of Nonholonomic Vehicles," *Proc. of IEEE International Conference on Robotics and Automation*, 2012, pp. 3206-3211.

[2] M. Krdhmiri, M. Keshmiri, "Performance comparison of various navigation guidance methods in interception of a moving object by a serial manipulator considering its kinematic and dynamic limits," *Proc. of 15th International Conference on Methods and Models in Automation and Robotics*, 2010, pp. 212-217.

[3] X. Anqi, G. Dudek, "Trust-driven Interactive Visual Navigation for Autonomous Robots," *Proc. of IEEE International Conference on Robotics and Automation*, 2012, pp. 3922-3929.

[4] J. Biswas, M. Veloso, "Depth Camera Based Indoor Mobile Robot Localization and Navigation," *Proc. of IEEE International Conference on Robotics and Automation*, 2012, pp.1697-1702.

[5] I. R. Manchester, M. L Emily, V. S. Andrey, "Vision-based interception of a moving target by a mobile robot," *Proc. of 16th IEEE International Conference on Control Applications*, 2007, pp. 397-402.

[6] I. R. Manchester, M. L Emily, V. S. Andrey, "Interception of a moving object with a specified approach angle by a wheeled robot: theory and experiment," *Proc. of IEEE Conference on Decision and Control*, December 2008, pp. 490- 495.

[7] J. A. Flores, S.R. Romo, O.I. Orozco, "Robot Rrafectory Planning for Multiple 2D Moving Object Interception: a Functional Approach," The Electronics, *Proc. of Robotics and Automotive Mechanics Conference*, 2006, pp. 77-82.

[8] F. Kunwar, B. Benhabib, "Rendezvous-Guidance Trajectory Planning for Robotic Dynamic Obstacle Avoidance and Interception," *IEEE Transactions on System, Man, and Cybernetics*, 2006, pp. 1432-1441.

[9] J. A. Flores, E. C. Dean, C. P. Montufar, "Operational Space Control Implemented in Robot Motion Planning for Multiple Objecs Interception Task," *Proc. of Electronics, Robotics and Automotive Mechanics Conference*, 2009, pp. 238-243.

[10] L. Freda, G. Oriolo, "Vision-based interception of a moving target with a nonholonomic mobile robot," *Robotics and Autonomous Systems*, Volume 55, Issue 6, 30 June 2007, pp. 419-432.

[11] F. Belkhouche, B. Belkhouche, P. Rastgoufard, "Line of Sight Robot Navigation Toward a Moving Goal," *IEEE Transactions on System, Man, and Cybernetics*, Vol. 36, No. 2, 2006, pp. 255-267.

[12] M. Hehn, R. Dandrea, "Real-time trajectory generation for interception maneuvers with quadrocopters," *Proc. of International Conference on Intelligent Robots and Systems*, 2012, pp. 4979-4984.

[13] K. G. Jolly, R. S. Kumar, R. Vijayakumar, "Intelligent task planning and action selection of a mobile robot in a multi-agent system through a fuzzy neural network approach," *Engineering Applications of Artificial Intelligence*, Vol. 23, Iss. 6, 2010, pp.923-933.

[14] K. G. Jolly, R. S. Kumar, R. Vijayakumar, "An artificial nerral network based dynamic controller for a robot in a multi-agent system," *Neurocomputing*, Vol. 73, Iss. 1-3, 2009, pp. 293-294.

[15] B. L. Chang, "A Trajectory Tracking Control Scheme Design for Nonholonomic Wheeled Mobile Robots with Low-level Control Systems," *Proc. of 2012 IEEE Conference on Decision and Control*, 2012, pp. 536-543.

[16] M. Farrokhsiar, H. Najjaran, "An Unscented Model Predictive Control Approach to the Formation Control of Nonholonomic Mobile Robots," *Proc. of IEEE International Conference on Robotic and Automation*, 2012, pp. 1576-1582.

[17] W. Budiharto, A. Santoso, D. Purwanto, A. Jazidie, "A navigation system for service robot using stereo vision and Kalman Filtering," *Proc. of 11th international conference on Control, Automation and Systems*, 2011, pp. 1771-1776.

[18] W. He, Y. Fang, X. Zhang, "The Study of a Vision-Based Pedestrian Interception System," *Proc. of 5th International Conference on Intelligent Robotics and Applications*, 2012, pp. 653-662.

[19] Y. Fang, X. Liu, X. Zhang, "Adaptive Active Visual Servoing of Nonholonomic Mobile Robots," *IEEE Transactions on Industrial Electronics*, Volume 59, Issue 1, 2012, pp. 486-497.